

1 **PLAM – A Meteorological Pollution Index for Air Quality and its**
2 **Applications in Fog-Haze Forecasts in North China**

3 **Yuanqin Yang¹, Jizhi Wang^{1*}, Sunling Gong^{1*}, Xiaoye Zhang¹, Hong Wang¹,**
4 **Yaqing Wang¹, Jie Wang², Duo Li³ and Jianping Guo¹**

5
6 1 Institute of Atmospheric Composition/Key Laboratory of Atmospheric Chemistry of
7 China Meteorological Administration (CMA), Chinese Academy of Meteorological
8 Sciences (CAMS), Beijing 100081, China

9 2 National Meteorological Information Centre, CMA, Beijing 100081, China

10 3 National Climate Centre, CMA, Beijing 100081, China

11
12 * Corresponding author: Sunling@cams.cma.gov.cn; wjz@cams.cma.gov.cn

13
14 **Abstract:** Using surface meteorological observation and high resolution emission data,
15 this paper discusses the application of PLAM/h Index (Parameter Linking Air-quality
16 to Meteorological conditions/haze) in the prediction of large-scale low visibility and
17 fog-haze events. Based on the two-dimensional probability density function diagnosis
18 model for emissions, the study extends the diagnosis and prediction of the
19 meteorological pollution index PLAM to the regional visibility fog-haze intensity. The
20 results show that combining the influence of regular meteorological conditions and
21 emission factors together in the PLAM/h parameterization scheme is very effective in
22 improving the diagnostic identification ability of the fog-haze weather in North China.
23 The **determination** coefficients for four seasons (spring, summer, autumn and winter)
24 between PLAM/h and visibility observation are 0.76, 0.80, 0.96 and 0.86 respectively
25 and all their significance levels exceed 0.001, showing the ability of PLAM/h to predict
26 the seasonal changes and differences of fog-haze weather in the North China region.
27 The high-value correlation zones are respectively located in Jing-Jin-Ji (Beijing,
28 Tianjin, Hebei), Bohai Bay rim and the southern Hebei-northern Henan, indicating that
29 the PLAM/h index has relations with the distribution of frequent heavy fog-haze
30 weather in North China and the distribution of emission high-value zone.
31 Comparatively analyzing the heavy fog-haze events and large-scale fine weather
32 processes in winter and summer, it is found that PLAM/h index 24 h forecast is highly
33 correlated to the visibility observation. Therefore, PLAM/h index has better capability

34 of doing identification, analysis and forecasting.

35

36 **Key Words:** meteorological condition, PLAM index method, fog-haze in North China,
37 diagnostic prediction

38

39 **1 Introduction**

40 Compared with 1980s, fog-haze pollution events have increased significantly in
41 the recent decade in the Beijing and North China region. Meteorological condition is
42 one of the important elements that impact the local aerosol accumulation and
43 contributes to the frequent appearance of low visibility weather (Wang et al., 2010,
44 Wang, et al., 2002). The synthetic impact analysis on the pollution-related atmospheric
45 dynamic, thermodynamic and chemical processes as well as the fog-haze prediction
46 study has drawn widely attentions. Long-term observations have pointed out that in the
47 last 30 years fog-haze phenomenon in the central and eastern part of China has become
48 more and more serious due to anthropogenic emissions. Under some meteorological
49 conditions, aerosol particles in the atmosphere can be activated into cloud condensation
50 nuclei (CCN), participating in the formation of clouds and fog, which means that
51 modern fog-haze have involved lots of polluted aerosol particles (e.g. $PM_{2.5}$). To
52 reduce the impact of the weather disaster of fog-haze, special attentions need to be
53 given to atmospheric aerosol pollution (Zhang, et al., 2013) The 3-dimensional
54 numerical model has been progressed in different degrees in the meteorological
55 services of the global air quality predictions(McKeen, 2007; Moran, 2009;
56 Zhang, 2009). Chemical forecasting model study and prediction usually faces the
57 problems of timely emission data all over the world, therefore limits the ability to
58 improve the forecasting accuracy. In recent years, through analyzing the observation
59 data of atmospheric aerosol particulate matter (PM) and the physical connection of
60 sensitive meteorological parameters, the establishment of air quality parameterized
61 diagnostic predicting method has being developed. Research results revealed that the
62 air quality meteorological index PLAM (Parameter linking Air-quality to
63 Meteorological conditions) can achieve reasonable results when it was applied in the
64 prediction of the air quality in Beijing during the 2008 Beijing Olympic Games. The
65 identification and prediction researches of meteorological condition PLAM index to air
66 quality have achieved progresses at home and abroad in recent years (Zhang et al.,

2009; Honoré et al., 2008; Li et al.; 2010; Kassomenos, et al., 2008; Yang, et al., 2009 ; Wang et al., 2013). Researches indicate that the contribution of meteorological condition PLAM index from emissions is of great importance as they have remarkable impacts on the regional distribution of air qualities in different areas. However, there are very limited researches on emission contribution to the air quality meteorological index, including its quantitative expression, physical mechanism and diagnostic prediction. This is especially critical in establishing the relations and mechanism of large-scale high-value PM_{2.5} and low visibility weather.

On the basis of parameterized meteorological condition principle method, this paper is to discuss the mutual impact of emission and meteorological condition, and study the structure and function of meteorological conditions PLAM index in quantitatively identifying, diagnosing and forecasting large scope of fog-haze weather.

2 Data and methods

This paper uses the near real-time (NRT) operational data, including surface observation data, from which the elements related to meteorological condition impact are extracted such as atmospheric temperature, difference of temperature and dew point, clouds, weather phenomenon, air pressure, wind direction and speed and visibility, and high-level sounding data as well as the data from atmospheric component observing system stations. The multi-source element data including high resolution emission data were analyzed to investigate the meteorological condition PLAM index identification method for forecasting wide-range low visibility and fog-haze.

2.1 Analysis on wet-equivalent potential temperature θ_e features of uniform air mass

Air quality and meteorological condition impacts are closely related. Usually different air mass structures can lead to significant difference of meteorological conditions. Studies pointed out that, aiming at the impact on air quality, it is very important to analyze and distinguish what kind of air mass controls and affects the local area, identify the differences of atmospheric aerosol features of the air masses in different types including maritime air mass, continental air mass or polar air mass etc., and consider the identification of stagnant air mass. The property of wet-equivalent potential temperature θ_e can be used to distinguish the types of air masses, because θ_e

100 includes dry and wet adiabatic processes, lifting condensation and sinking and other
 101 dynamic and thermodynamic processes in atmosphere, having the property of
 102 conserving and being able to be tracked and identified. The equation of wet-equivalent
 103 potential temperature is:

$$104 \quad \theta_e = \theta \exp\left[\left(\frac{Lw}{C_p T}\right)\right] \quad (1)$$

$$105 \quad \text{where: } \theta \text{ is potential temperature: } \theta = T \left[\left(\frac{1000}{P}\right)^{\frac{R_d}{C_p}} \right] \quad (2)$$

106 the unit of θ and θ_e is °K. w , C_p , L , R_d , P and T are mixing ratio,
 107 constant-pressure specific heat ($C_p=1.005 \text{ J}^*\text{g}^{-1}*\text{degree}^{-1}$), latent heat of
 108 condensation of water vapor ($L = 2500.6 \text{ J}^*\text{g}^{-1}$), gas constant ($R_d = 2.87*10^{-1}$
 109 $\text{J}^*\text{g}^{-1}*\text{degree}^{-1}$), air pressure and temperature, respectively.

110

111 **2.2 Parameterized method of diagnosing and forecasting atmospheric process**

112 The interactions and mutual effects of atmospheric micro-physical process and
 113 large-scale process as well as the different scales of process are very complicated in
 114 the transient of cloud and fog physical process as well as the atmospheric pollution
 115 process. The meaning and main idea of the parameterized method is to connect the
 116 non-linear relationship that is difficult to describe in the processes of different scales
 117 with a parameterization scheme. Studies (Kuo, 1961; Kuo,1965; Kuo, 1974) have
 118 shown that the micro-processes in cloud physics can be described in a
 119 parameterization scheme with the large-scale observations. Based on the Lagrangian
 120 method the variation of fluid particle group going with time can be followed, i.e.,
 121 identifying the “stagnant and less changing” state of air masses. In the atmospheric
 122 particle movement, the individual change of wet-equivalent potential temperature
 123 (spatial-temporal total derivative) gets to a small value or zero, meaning little
 124 changes. Therefore, according to the identification of the “stagnant and less
 125 changing” property of wet-equivalent potential temperature of air masses, i.e., the
 126 basic physical process of $\frac{d\theta_e}{dt} \approx 0$, the possible varying trend of air quality of the

127 “stagnant and less changing” air masses can be diagnosed and predicted. The
 128 recently developed air quality diagnosis of parameterized meteorological conditions
 129 (Yang, et al., 2009 ; Zhang, et al., 2009; Wang, et al., 2012) PLAM index is described
 130 as follows:

$$131 \quad \text{PLAM}_0 = \frac{d\theta_e}{dt} \cong \theta_e \frac{f_c}{C_p T} \quad (3)$$

132 θ_e is wet-equivalent potential temperature given out by Eq.(1). f_c is wet air
 133 condensation rate:

$$134 \quad f_c = f_{cd} / \left[\left(1 + \frac{L}{C_p} \frac{\partial q_s}{\partial T} \right)_p \right] \quad (4)$$

135 f_{cd} is dry air condensation rate:

$$136 \quad f_{cd} = \left[\left(\frac{\partial q_s}{\partial P} \right)_T + \gamma_p \left(\frac{\partial q_s}{\partial T} \right)_p \right] \quad (5)$$

$$137 \quad \gamma_p \text{ is dry-adiabatic lapse rate: } \gamma_p = \frac{R_d * T}{C_p P} \quad (6)$$

138 q_s is specific humidity. The meanings of other variables are the same as the
 139 above-mentioned.

140 The Eq.(3) shows that the parameterized method based on the spatial-temporal
 141 variation of wet-equivalent potential temperature of air masses has practical application
 142 prospect in analyzing, diagnosing and forecasting the changes of air quality. The
 143 objective of this paper is to further discuss the impact and identification of PLAM_0
 144 index to aerosol pollution concentration accumulative increase and atmospheric
 145 fog-haze weather, and moreover study the possibility of using the parameterized
 146 method to improve the diagnosing and forecasting capability to large-scale disastrous
 147 fog-haze weather.

148

149 **2.3 Contribution and impact of atmospheric emission on PLAM index**

150 Considering the diagnosis and forecasting analysis of atmospheric fog-haze which is
 151 closely related to atmospheric aerosols (such as fine particle $\text{PM}_{2.5}$ etc.), it is very
 152 important to integrate the effect of the initial meteorological conditions PLAM_0 and

153 emission contribution. In order to integrate the initial meteorological condition related
 154 to atmospheric pressure, temperature, humidity, condensation, etc. with the
 155 contribution of the pollutant emission factor p in the atmosphere, the identification
 156 parameter was expressed by Eq. (7) (Wang et al., 2012) :

$$157 \quad \text{PLAM_haze} = \text{PLAM}_0 \times p \quad (7)$$

158 This factor p further expands the application of PLAM index and investigates the
 159 description of the function and impact of the index by emissions in the forming and
 160 developing process of regional wide-range fog-haze event, namely PLAM_haze
 161 (abbreviated as PLAM/h). Thus, analysis on the latest emission research results as of
 162 2010 is introduced including industry, energy source, transportation, anthropogenic
 163 emission source combined $E_{\text{PM}_{2.5}}$ (Unit: tons *10)(Figure 1a). It is seen from Figure 1a
 164 that the high-value zones from industry, energy source, transportation and
 165 anthropogenic emission source in the North China region involve ① the central and
 166 southern part of Hebei (including Beijing and Tianjin), ② the central and western part
 167 of Shandong, ③ the central part of Henan, ④ the eastern part of Hubei, ⑤ the Yangtze
 168 River delta and ⑥ the eastern part of Sichuan (the Chengdu Plain). All these
 169 high-value emission sources have significant impacts on the fog-haze weather in North
 170 China and cannot be underrated.

171 To quantify the impact of emission in PLAM index, the probability of its impact
 172 on the surrounding area satisfies the normal distribution, that is, by separating the
 173 impacts of meteorological condition and emission on the surrounding part, it is always
 174 isotropic and the impact probability of high emission center area is higher than that of
 175 the surrounding area. As a result, the emission impact satisfies the form of
 176 2-dimensional probability distribution, and the integral probability density function that
 177 falls into the surrounding limited area x, y plane (s) is as follows:(Wang et al, 1985 ;
 178 Neumann et al., 1978):

$$179 \quad P(s) = \iint_s f(x, y) dx dy = 1 - \exp(-\gamma^2/2) \quad (8)$$

180 where γ is the standardized (normalized) grade of the emission source intensity in the
 181 concerned forecasting area, $\gamma \in (0, 1)$, defined as $\gamma = (E - E_{\min}) / (E_{\max} - E_{\min})$, where E_{\max}
 182 and E_{\min} are the maximum value and minimum value of the emission E in the specified
 183 season of the studied impact region (North China). In other words, the exponential

184 growth rate with emission impact is $P=1+P'$. Then, the impact of emission on the
185 increase value of fog-haze is taken into account, and the Eq. (3) can be formulated into:

$$186 \quad \text{PLAM} = \theta_e \frac{f_c}{C_p T} \times P(\gamma) \quad (9)$$

187 **3 Results and Discussion**

188 **3.1 Analysis on PLAM index medium emission contribution features**

189 Studies pointed out that emission does not change very much in certain fixed temporal
190 scales (such as a month or a season) in the same area, but differs greatly in different
191 places. To analyze the contribution of regional emission on the low visibility weather
192 like fog-haze, the comparable standardized emission intensity (γ) in the regional and
193 seasonal period was calculated based on the meteorological observation data in
194 different places and different time periods. Figure1a presents the distribution of high
195 resolution emission lists. Figure1b is the standardized distribution of emission list in
196 the North China region based on Figure1a. From Figure 1b, it can be seen that ①
197 Beijing, Tianjin and the central and southern part of Hebei, ② the west of Shandong,
198 ③ the central part of Henan, ④ the eastern part of Hubei, ⑤ the Yangtze river delta
199 and ⑥ the east of Sichuan remain to be the significantly concentrated high emission
200 regions, whose circular or oval-shaped distribution characteristics are clearly seen.
201 Taking the rarely-seen large-range heavy fog-haze weather event over Beijing and the
202 North China region on 26 February 2014 as an example, the difference by considering
203 and ignoring the emission contribution in PLAM index is discussed. Figure1c and d
204 show the PLAM index distribution under the condition of considering and ignoring the
205 emission in North China at 08:00 (UTC+8) 26 February 2014. It is seen from the figure
206 that under the condition without considering the emission impact (Figure1c) the
207 distribution centers of PLAM index are: Hebei, Beijing-Tianjin region in North China;
208 southern Hebei, northern Henan; western Hubei and northern Sichuan. The PLAM
209 indices are 120, 160, 160 and 80 (Figure.1c) respectively. Figure1d shows PLAM/h
210 distribution with the emission impact. The above-mentioned four PLAM/h index high
211 value zones are 180, 180, 180 and 160, respectively. The PLAM/h value increases
212 along with the significant expansion of high-value (the green oval-shaped circle in the
213 figure).

214 To further discuss the difference, Figure2 displays the correlation analysis of 24
215 h forecasting and visibility of PLAM/h index at 673 stations in North China on

216 26 February 2014. For the convenience to compare, the overlap of the correlati
217 on distributions of PLAM/h and visibility under the condition of including and
218 excluding emission factors is given out. The considered emission in Figure 2 is
219 expressed by blue triangle while the ignored emission is marked with red circl
220 e -- yellow filled circle. The correlation fitted lines are respectively marked by
221 red solid line and yellow dashed line. It is seen from Figure 2 that the reasona
222 ble correlation exists between PLAM/h and visibility on 26 February 2014 regar
223 dless of emission contributions. However, determination coefficient (R^2) is increa
224 sed from 0.3675 to 0.3887 when emissions are considered, indicating the import
225 ance of inclusion of emission in PLAM/h.

226

227 It is noted that in the low-value visibility range ($Vis < 10\text{km}$), the PLAM/h index
228 value without emission impact shifts towards low-value zone clearly. Comparatively,
229 the closer to the high-value zone of visibility, the more the two types of symbols tend
230 to overlap, which suggests that, without emissions, the predictive value of PLAM/h
231 index will be smaller and its correlation with visibility will be reduced, deviating the
232 fitted low-value zone line.

233 In summary, the above analyses on the regional PLAM/h distribution (Figure 1)
234 and the correlation distribution of PLAM/h and visibility (Figure 2) all indicate that
235 with the combined impact of meteorological condition and emission factors, the
236 description capability of PLAM/h index increases significantly with the index value
237 expanding to the high-value zone; the PLAM/h index including the emission has
238 obvious impact on improving the capability of diagnosing and identifying the heavy
239 fog-haze weather.

240

241 **3.2 Analysis on seasonal characteristics of PLAM/h index and visibility** 242 **correlation**

243 Figure 3 separately presents distribution of fog-haze weather in the typical heavy
244 fog-haze process cases in four seasons, including the PLAM/h (a) and visibility (b) of
245 the 14 April 2011 spring case, the PLAM/h (c) and visibility (d) of the 26 July 2008
246 summer case, the PLAM/h (e) and visibility (f) of the 30 October 2011 autumn case
247 and the PLAM/h (g) and visibility (h) of the 7 January 2011 winter case.

248 In spring, the PLAM/h index low-value zone on 14 April 2011 is mainly in the

249 North China region. 3/4 regional PLAM/h < 70 in the whole region. The
250 meteorological condition is good for pollutants to diffuse. There is a weak PLAM/h
251 relatively high-value zone across the central Henan, southern Hebei, Beijing-Tianjin
252 and northern Hebei, which is PLAM/h ≥ 80. Besides, there is another high-value zone in
253 the coastal parts of Bohai Sea, corresponding to the sea fog prone area in the southern
254 part of North China. The PLAM/h high value matches with the low-value zone of
255 visibility whilst the large-range PLAM/h low-value zone goes with the high-value zone
256 of visibility.

257 In Summer, the 08:00(UTC+8) 26 August 2008 case shows that the North China
258 region is a large-scale PLAM/h high-value zone, whose center distributes in
259 north-south banding shape: ① East of Taihang Mountains in Henan province to
260 southern Hebei (PLAM/h value is 120 and the highest even gets to 200), ② Beijing
261 and central Hebei (PLAM/h value is 120-140), ③ the Jing-Jin-Tang (Beijing, Tianjin,
262 Tangshan) region (PLAM/h value is high up to 120-240) and ④ the west-southern
263 Shandong (PLAM/h value reaches 140-200) are four remarkable banding high value
264 centers. Corresponding to the wide-range low visibility low value zones, the visibility
265 in most parts is lower than 10 km, of which the visibility from Henan to southern Hebei
266 is lower than 4 km. The Beijing-Tianjin region has the visibility of 4-8 km only. So,
267 PLAM/h index has significant effect on diagnosing and identifying the summer
268 fog-haze weather in North China.

269 North China usually has clear and refreshing autumn weather. But in recent years,
270 heavy fog-haze weather events appear more and more frequently in autumn. To
271 examine the identifying capability of PLAM/h index in the typical autumn heavy
272 fog-haze case, we analyze the rarely seen heavy fog-haze pollution process that
273 happened in North China on 30 October 2011. According to Figure 3g and 3h, the
274 high-value PLAM/h index in the fog-haze area in North China assumes in the
275 north-south trend parallelized to the regional distribution of three large-scale bands (3g)
276 and PLAM/h > 200-240, of which the three high-value PLAM/h bands are parallel to
277 the Taihang Mountains in North China, orderly arranged along the line of the boundary
278 between Shanxi and Hebei-southern Liaoning (dotted line in the figure) and being
279 greatly consistent with the banding distribution of the fog-haze and low visibility areas
280 in North China (Figure 3h). The large scope of PLAM/h low-value zone, PLAM/h <
281 20-50, in the western and northern parts of North China agrees with the high-value

282 visibility zone with $Vis > 20\text{km}$. Therefore, PLAM index has the characteristics of
283 weather-scale banding distribution similar to the distribution of weather systems.

284 One heavy fog-haze process rarely seen in history appeared in North China in the
285 first-half month of January 2013. This is a typical winter heavy fog-haze case, whose
286 PLAM/h index is significantly high, indicating the contribution of meteorological
287 condition to the enhancement and persistence of this large-range fog-haze process is
288 dominating. PLAM/h index high-value zone blankets the Beijing-Tianjin, the east to
289 Taihang Mountains to the most part of North China which is to the south of Yanshan
290 Mountains. The banding fog-haze weather area in the southwest-northeast trend
291 extends eastward into the southern part of Liaoning. Corresponding to the
292 southwest-northeast trend banding high-value zone of PLAM/h index (Figure 3g), the
293 visibility is the accordant banding low-value distribution area (Figure 3h)

294 The seasonal results analysis of PLAM/h index shows its characteristics linkage
295 with weather-scale system in each season. The weather-scale high-value PLAM/h zone
296 agrees with the low-value visibility area, which indicates the regional distribution of
297 PLAM/h index is indicative of diagnosing, identifying and forecasting the large-range
298 fog-haze area in four seasons in North China.

299 Figure 4 reveals the correlation of PLAM/h index and visibility in different
300 seasons which is calculated by Eq. (9) according to the 2009 daily observation data in
301 Beijing. As the seasonal features related to aerosol pollution in North China are
302 different from the seasonal features divided according to temperature elements, the
303 selected representative stations are slightly different. For the analysis of this paper, the
304 season from July to August is defined as rainy season or summer and from November
305 to the next February is winter in North China. Spring and autumn are two transition
306 seasons, taking March to June and September to October respectively. In Figure 4a the
307 chosen period of winter includes January-February and November-December of
308 Beijing (BJ) and Zhengzhou (ZZ), there are totally 240 groups of observation record.
309 In Figure 4b there are totally 248 groups of observation records chosen for the summer
310 July-August of Beijing (BJ), Zhengzhou (ZZ), Taiyuan (TY) and Jinan (JN). Figure 4c
311 involves 122 groups of records from Beijing (BJ) for the season of spring March-June.
312 Figure 4d contains 122 groups of observation records for the autumn
313 September-October of Beijing (BJ) and Zhengzhou (ZZ). It is seen from the figures
314 that:

- 315 1) The variation of air quality meteorological condition PLAM/h index is significantly
316 correlated to the visibility observation (Vis) in Beijing and the **determination**
317 coefficients (R^2) are 0.8587 (winter), 0.8009 (summer), 0.7617 (spring) and 0.9552
318 (autumn), respectively, with all significance levels exceeding 0.001.
- 319 2) In winter (Figure 4a), with the low-value meteorological condition index, when
320 $PLAM/h < 80$, $Vis > 25$ km; when high value of PLAM/h gets up to 150-350, the
321 observed visibility trend gets worse with $Vis < 10$ km. Different from winter,
322 during the low-value meteorological condition index in summer, when $PLAM <$
323 **150**, $Vis >$ **10** km; when the PLAM high value rises to 150, the observed visibility
324 becomes worse and $Vis < 5$ km (Figure 4b). This means that PLAM/h has
325 significant capability to describe optimal or inferior visibility, and, moreover, its
326 seasonal difference is great. This finding is consistent with the climate observation
327 result that the aerosol concentration high value in summer appears at the same pace
328 with low visibility(Wang, 2006).
- 329 3) Figure 4 shows that the correlations in the two transition seasons are noticeably
330 different. The correlation features in spring are similar to those in summer while
331 the autumn features are like winter's. But during the transition seasons, spring and
332 autumn, the threshold value deduced from the diagnosis of PLAM/h to heavy
333 fog-haze pollution is lower, that is, when the meteorological condition index
334 PLAM/h gets to 150, visibility is with very low value, even $Vis < 5$ km.

335 In summary, the above analyses indicate that PLAM/h is capable to describe the
336 changes of visibility, and also capable of distinguishing the seasonal differences very
337 well. The seasonal threshold difference resulting from the diagnosis of PLAM/h to
338 heavy fog-haze pollution is indicative of quantitatively identifying and diagnosing the
339 appearance of fog-haze pollution.

340

341 **3.3 PLAM index and related features of visibility area**

342 Figure 5 shows the regional correlation between PLAM/h index and visibility which is
343 obtained by calculating the 1006 groups of observation samples collected from January
344 2009 to December 2012, **the icon for 0-100%, drawing the R^2 value magnified by 100**
345 **in Fig.5**. The regional distribution of the correlation with significance level exceeding
346 0.001 is also shown. The figure indicates that most part of North China is the
347 high-value zone $> 80\%$, of which one high-value zone is located in Shanxi, most

348

349

350 Mountains in North China as well as the distribution of high emission areas in southern
351 Hebei and northern Hubei (Figure 1b) ; another high correlated zone which sits in
352 Beijing-Tianjin and the Bohai Bay rim is possibly related to the weather condition of
353 the more fog-haze “back-flow” of the easterly wind in North China. These analyses
354 suggest that the North China PLAM/h and index features are significantly correlated to
355 visibility, the high correlation area with significance level exceeding 0.001 is likely
356 related to the regional distribution of meteorological condition of heavy fog weather in
357 North China and the distribution of regional emission high-value zone in North China.

358

359 **3.4 Application of PLAM/h index in fog-haze forecasting**

360 **3.4.1 The 20-26 February 2014 winter case analysis**

361 Applying the PLAM/h index developed in this paper, 24 h forecasts of visibility with
362 PLAM/h are conducted for one historically rarely-seen winter heavy fog-haze process
363 in North China during the last half of February 2014 (20-26 February 2014). During
364 the test , the NRT data of more than 670 stations in the North China region are adopted
365 to analyze the correlation between PLAM/h index 24 h forecasts and visibility
366 observation. Figure 6a and b reveal the correlation analysis results of PLAM/h index
367 24 h forecasts and observed visibility respectively at 08:00 (UTC+8) 20 and 08:00
368 (UTC+8) 22 February 2014. Table 1 lists the correlation of daily PLAM/h index 24 h
369 forecasts and visibility during the whole process of the regional heavy fog-haze event
370 over North China in 20-26 February 2014 as well as the number of stations that are
371 involved in the test.

372 From Figure 6 and Table 1 it can be seen the daily **determination** coefficients (R^2)
373 are 0.6529, 0.5424, 0.6047, 0.6040, 0.4550 and 0.3887, respectively; the significance
374 levels all pass 0.001, which means their correlation is very good.

375

376

377 **3.4.2 The 19-22 July 2013 summer case analysis**

378 To further investigate the forecasting capability of summer PLAM/h index to the
379 fog-haze area distribution, forecast application and testing analysis of one heavy
380 fog-haze pollution process in North China in summer 19-22 July 2013 are carried out.
381 On 19 July, extremely heavy fog emerged in the day time over Beijing, just as night

382 had fallen. It was very dark with local visibility less than 5 m. Figure 7a and b reveal
383 the correlation analysis result of PLAM/h index 24 h forecast and visibility during the
384 polluting process in the North China region respectively at 08:00 (UTC+8) 20 and 22
385 July 2013. Table 2 presents the correlation of daily PLAM/h index 24 h forecast and
386 visibility during the whole process of the regional heavy fog-haze event over North
387 China in 19-22 July 2013 as well as the number of stations that participate in the
388 forecasting test. From Figure 7 and Table 2, the daily determination coefficients (R^2)
389 respectively are 0.4988, 0.4826, 0.5416 and 0.5263, and all their significance levels
390 exceed 0.001.

391 The above analyses indicate that the PLAM/h index 24 h forecasts and visibility
392 observations of the large-range samples in different winter and summer over North
393 China all have higher correlations. This result illustrates the PLAM/h index would have
394 good practical application prospect in forecasting the regional large-scale fog-haze
395 weather in North China.

396

397 **3.4.3 The 12 March 2014 fine weather case analysis**

398 In order to investigate the analysis and identification capability of PLAM/h to
399 the fine and sunny weather without fog or haze, the correlation between PLAM/h and
400 visibility in a wide range of fine weather has been carried out. As an example, Figure
401 8a and b reveal the correlation analysis of the regional PLAM/h distribution and
402 PLAM/h index 24 h forecasts on 12 March 2014.

403 It is seen from Figure 8a that most part of North China has low-value PLAM/h
404 < 60 (blue area in the figure). The meteorological condition PLAM/h index
405 distribution displays that large area of North China lies in the area with the
406 meteorological condition extremely favorable for atmospheric dispersion. Beijing is
407 under blue sky with clouds. The PLAM/h index forecasts of Beijing and Baoding
408 (Hebei) are 53 and 29 respectively. From daytime to evening on 12 March, the $PM_{2.5}$
409 value of Beijing urban area is reported to be 21-35 $\mu\text{g}/\text{m}^3$.

410

411 Figure 8b is the correlation analysis of PLAM/h index 24 h forecasts and
412 observed visibility at 677 stations in North China on 12 March 2014, which was made
413 based on real-time data. It can be seen that the determination coefficient (R^2) gets to
414 0.412 and the significance level passes 0.001 averagely. On 13 March 2014, Beijing

415 continues to enjoy the clear weather with blue sky and clouds, so air quality is
416 excellent. The $PM_{2.5}$ value of Beijing urban area still remains at high level of
417 22-37 $\mu\text{g}/\text{m}^3$. The above analysis indicates that for large-scale fine weather or
418 low-visibility heavy pollution weather, PLAM/h index has the strong capability of
419 identifying, analyzing and forecasting.

420

421 **4. Conclusions**

422

423 PLAM – A meteorological pollution Index for air quality has been developed and used
424 in NRT air quality forecasts, by considering both meteorology and pollutant emissions.
425 Based on the emission diagnosing model of 2-dimensional probability density function,
426 the paper has extended the parameterized description of original PLAM, applying it in
427 the diagnosis and forecasting of the variation and distribution of wide-range regional
428 low-visibility fog-haze intensity and achieving satisfactory results. The contrast
429 analysis with or without the emission impact indicates that meteorological condition
430 and emission factor jointly play the role in expanding PLAM towards high-value zone.
431 This means that PLAM/h index involving emission has significant effect on improving
432 the capability of diagnosing and forecasting heavy fog-haze weather in North China.

433 The variation of air quality meteorological condition index PLAM/h is
434 significantly correlated to the regional visibility observations in North China. The
435 **determination** coefficients of winter, summer, spring and autumn are 0.8557 (winter),
436 0.8009 (summer), 0.7617 (spring) and 0.9552 (autumn), respectively and their average
437 significance level goes beyond 0.001.

438 The correlation analysis of index and visibility regional distributions indicates that
439 the high correlation zones respectively lie in Jing-Jin-Ji (Beijing, Tianjin, Hebei),
440 Bohai Bay rim, southern Hebei and northern Hubei. This indicates that PLAM/h index
441 is related to the distributions of the North China weather system and the heavy fog
442 occurrence region as well as the distribution of emission high value zones, which is
443 indicative to diagnose and identify the regional distribution of the fog-haze frequently,
444 hit areas.

445 The analyses on typical high pollution cases of spring, summer, autumn and winter
446 suggest that PLAM/h index regional distribution is related to the banding distribution
447 features of weather-scale systems in different seasons. The weather-scale high-value
448 PLAM/h areas correspond to the low-visibility areas, indicating the PLAM/h index has

449 the diagnosing, identifying and forecasting capability to the wide-range fog-haze areas
450 and their seasonal differences in North China.

451 Although winter is different from summer, the PLAM/h index 24 h forecasts and
452 visibility observations from the weather stations of North China, including wide-range
453 fine weather and the low-visibility heavy pollution weather, all have high correlations.
454 This indicates the PLAM/h index has good identifying, analyzing and forecasting
455 capabilities. These conclusions show that the PLAM/h index will have good practical
456 application prospect in forecasting the large-scale fog-haze areas and their seasonal
457 differences in North China.

458

459 *Acknowledgements*

460 This work was funded by the National Key Foundation Study Developing
461 Programm (2011CB403404,2011CB403401), National Key Technology R&D Program
462 (Grant no. 2014BAC16B01) National Natural Science Foundation of China under
463 Grant (No. 41275167, No. 41275007) and CMA Innovation Team for Haze-fog
464 Monitoring and Forecasting

465

466 References

467 Gong, S.L., Barrie, A., Blanchet, J.P., Salzen, K. N, Lohmann, U., Lesins, G.,
468 Spacek, L.,Zhang, L.M., Girard, E., Lin, H., Leaitch, R., Leighton, H., Chylek, P.,
469 Huang, P.: Canadian aerosol module: a size-segregated simulation of atmospheric
470 aerosol processes for climate and air quality models 1. Module development J.
471 Geophys. Res. 108, 4007-4015, 2003.

472 Honore', C., Rouil, L., Vautard, R.: Predictability of European air quality:
473 Assessment of 3 years of operational forecasts and analyses by the PREV'AIR system.
474 J. Geophys. Res.,113: D04301,4302-4310, 2008.

475 Kassomenos, P., Papaloukas, C., Petrakis, M., Karakitsios, S.: Assessment and
476 prediction of short term hospital admissions: the case of Athens, Greece. Atmos. Environ.
477 42 (30), 7078-7086, 2008.

478 Kuo,H.L.: Convective Weather in Conditionally Unstable Atmosphere, Tellus, 13,
479 441-459, 1961.

480 Kuo,H.L.: On Formation and Intensification of Tropical Cyclone through Latent
481 Heat Release in Cumulus Convection, J .Atmos. Sci 22,40-23,1965.

482 Kuo,H.L.:Further Studies on the Parameterization of the Influence of Cumulus
483 Convection in Large-scale Flows, J. Atmos. Sci. 31,1232-1240, 1974.

484 Li, Y., Wang, W., Wang, J.Z., Zhang, X.L., Lin, W.L., Yang, Y.Q.: Impact of air
485 pollution control measures and weather conditions on asthma during the 2008 Summer
486 Olympic Games in Beijing. Int. J. Biometeorol.. [http://dx.doi.org/
487 10.1007/s00484-010-0373-6](http://dx.doi.org/10.1007/s00484-010-0373-6), 2010.

488 McKen, S.: Evaluation of several real-time PM2.5 forecast models using data
489 collected during the ICARTT/NEAQS 2004 field study, J. Geophys. Res. 112: D10S20,
490 DOI: 10.1029/2006JD007608,2007.

491 Moran, M.D.:on particulate matter formation in the Mediterranean Region. In
492 Proceedings of the 30th NATO/SPS ITM on Air Pollution Modelling and Its
493 Application, (San Francisco), 2009.

494 Neumann C. J.,Mandal, G. S.: Analog forecasting methods of tropical cyclones in
495 India ocean. Indian J Met. Geophys.,29(3):487-500,1978.

496 Rigby, M., Toumi, R.: London air pollution climatology: indirect evidence for
497 urban boundary layer height and wind speed enhancement. Atmos. Environ. 42 (20),
498 4932-4947. 2008.

499 Wang, J. Z., Gong, S. L., Zhang, X. Y.,Yang,Y. Q. Hou, Q., Zhou,C.H., and

500 Wang, Y.Q.: A parameterized method for air-quality diagnosis and its applications.
501 Adv Meteorol, Article ID 238589: 1-10,doi:10.1155/2012/238589, 2012.

502 Wang,J.L.,Liu, X.L.: The Discuss on relationship between visibility and mass
503 concentration of PM_{2.5} in Beijing, Acta Meteorlo Sin, 64 (2) ,221-228,2006.

504 Wang J.Z., Neumann, C. J.: A Markov-type analogmedel for prediction of
505 typhoon motion in Northwestern Pacific, Scientia Sinica (Series B),28(5):517-526,
506 1985. Wang,J.Z., Wang, Y.Q., Liu, H., Yang, Y.Q., Zhang,X.Y., Li, Y., Zhang, Y.
507 M., Deng, G.:Diagnostic identification of the impact of meteorological conditions on
508 PM_{2.5} concentrations in Beijing Atmospheric Environment, 81 158-165, 2013.

509 Wang, J.Z., Yang, Y.Q., Zhang, G.Z., Yu, S.Q.: Climatic trend of cloud amount
510 related to the aerosol characteristics in Beijing during1950-2005, Acta Meteorol. Sin.
511 24 (6), 762-775, 2010.

512 Wang J. Z., Xu, X. D., Yang, Y.Q.: A studyof characteristics of urban visibility
513 and fog in Beijing and the surrouding area(in Chinese), Journal of Applied
514 Meteorological Science Suppl 13: 160-168, 2002.

515 Yang,Y.Q., Wang,J. Z., Hou, Q., Wang,Y. Q.: A Plam Index for Beijing
516 Stabilized Weather Forecast in Summer Over Beijing. Journal of Applied
517 Meteorological Science 20, 649-655, 2009.

518 Zhang, X. Y., Sun, J. Y., Wang, Y. Q., Li, W. J., Zhang, Q., Wang, W. Z., Qian, J.
519 N.,Cao, G. L., Wang, J. Z., Yang, Y. Q., Zhang, Y. M.: Factors contributing to haze
520 and fog in China (in Chinese), Chin Sci Bull (Chin Ver), 58: 1178–1187,doi:
521 10.1360/972013-150,2013.

522 Zhang, X.Y., Wang, Y.Q., Lin, W.L., Zhang, Y.M., Zhang, X.C., Gong, S.L.,
523 Zhao, P., Yang, Y.Q., Wang,J.Z., hou, Q., Zhang, X.L., Che, h. Z., Guo, J.P., Li, Y.:
524 Changes of atmospheric composition and optical properties over Beijing 2008 Olympic
525 Monitoring Campaign. Bull. Am. Meteorol. Soc. 90 (11), 1633-1649, 2009.

526

527

528

529

530

531

532

533

534 **Figure captions**

535 Figure 1 High resolution emission list E distribution (a) and its regional emission
536 standardized list γ (b); PLAM index distribution with ignoring (c) and considering (d)
537 the emission condition in North China at 08:00 (UTC+8) 26 February 2014

538 Figure 2 Correlation analysis of PLAM and visibility considering and not considering
539 emission factors on 26 February 2014

540 Figure 3 The cases for PLAM/h (a) and visibility (b) of the 14 April 2011 , PLAM/h (c)
541 and visibility (d) of the 26 July 2008, PLAM/h (e) and visibility (f) of the 30 October
542 2011 and PLAM/h (g) and visibility (h) on 7 January 2011

543 Figure 4 Correlation analysis of PLAM/h index and visibility in winter (a), summer (b),
544 spring (c) and autumn (d)

545 Figure 5 the regional correlation between PLAM/h index and visibility obtained by
546 calculating the 1006 groups of observation samples collected from January 2009 to
547 December 2012. The regional distribution of the correlation with significance level
548 exceeding 0.001

549 Figure 6 the correlation analysis results of PLAM/h index 24 h forecasts and observed
550 visibility respectively at 08:00 (UTC+8) 20(a) and 08:00 (UTC+8) 22(b) February
551 2014

552 Figure 7 Correlation analysis of the regional PLAM/h index 24 h forecasts and
553 visibility during the whole period of pollution in North China respectively at
554 08:00(UTC+8) 20(a) and 08:00(UTC+8) 22 July 2014(b)

555 Figure 8 distribution of PLAM/h in North China (a)and the correlation analysis of
556 PLAM/h index 24 h forecasts and observed visibility in North China for
557 8:00(UTC+8) March 12, 2014 (b)

558

559 Table 1 Correlation of daily PLAM/h index 24 h forecasts and visibility during the
560 whole process of the regional heavy fog-haze event over North China in 20-26
561 February 2014

562

563

564

565

566

| Forecast time | determination coefficient (R ²) | Station number |
|-----------------------|---|----------------|
| 08 :00(UTC+8) 20 Feb. | 0.6529 | 674 |
| 08 :00(UTC+8) 21 Feb. | 0.5424 | 668 |
| 08 :00(UTC+8) 22 Feb. | 0.4634 | 669 |
| 08 :00(UTC+8) 23 Feb. | 0.6047 | 676 |
| 08 :00(UTC+8) 24 Feb. | 0.6040 | 673 |
| 08 :00(UTC+8) 25 Feb. | 0.4550 | 678 |
| 08 :00(UTC+8) 26 Feb. | 0.3887 | 673 |

574

575

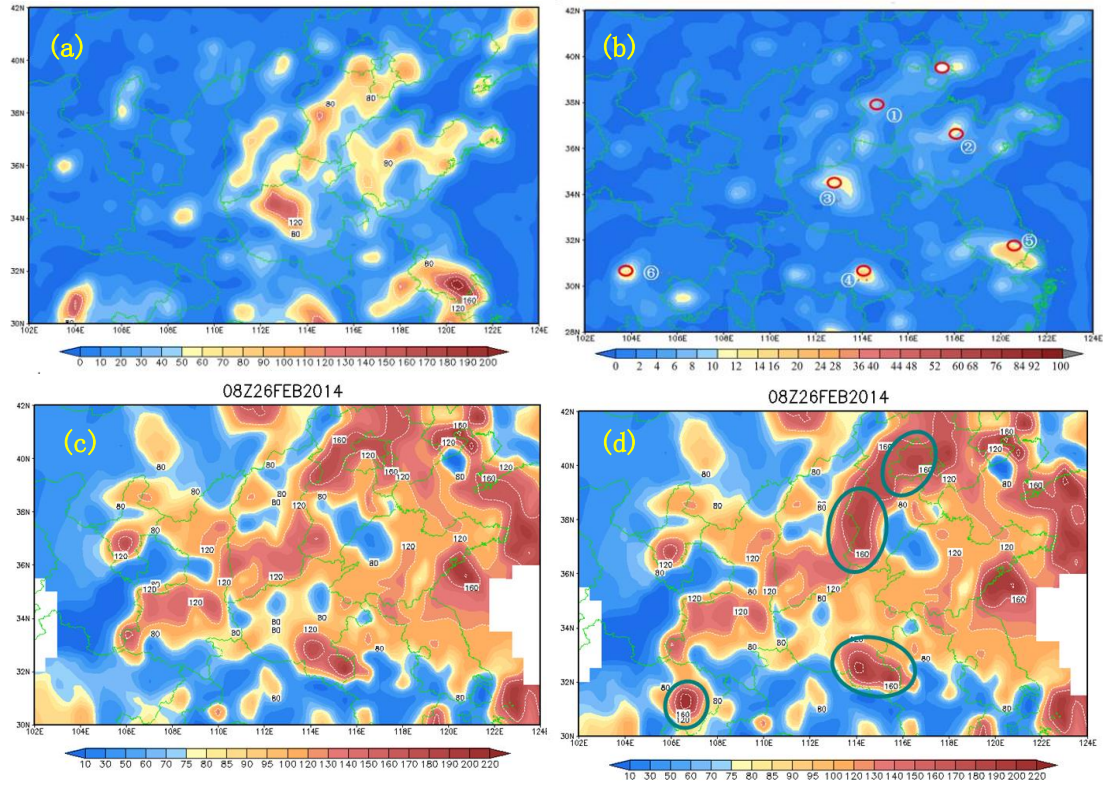
576 Table 2 Correlation of daily PLAM/h index 24 h forecasts and visibility during the
 577 whole process of the regional heavy fog-haze event over North China in 19-22 July
 578 2013

579

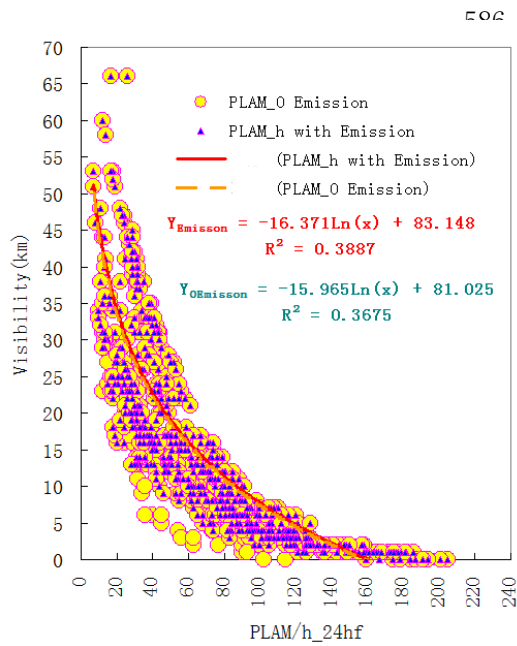
| Forecast time | determination coefficient (R ²) | Station number |
|--------------------------|---|----------------|
| 08 :00(UTC+8) 19 Jul. | 0.4988 | 682 |
| 08 :00(UTC+8) 20 Jul. | 0.4826 | 683 |
| 08 :00(UTC+8) 21 Jul. | 0.5416 | 685 |
| 08 :00(UTC+8) 22 Jul. | 0.5263 | 181 |

580

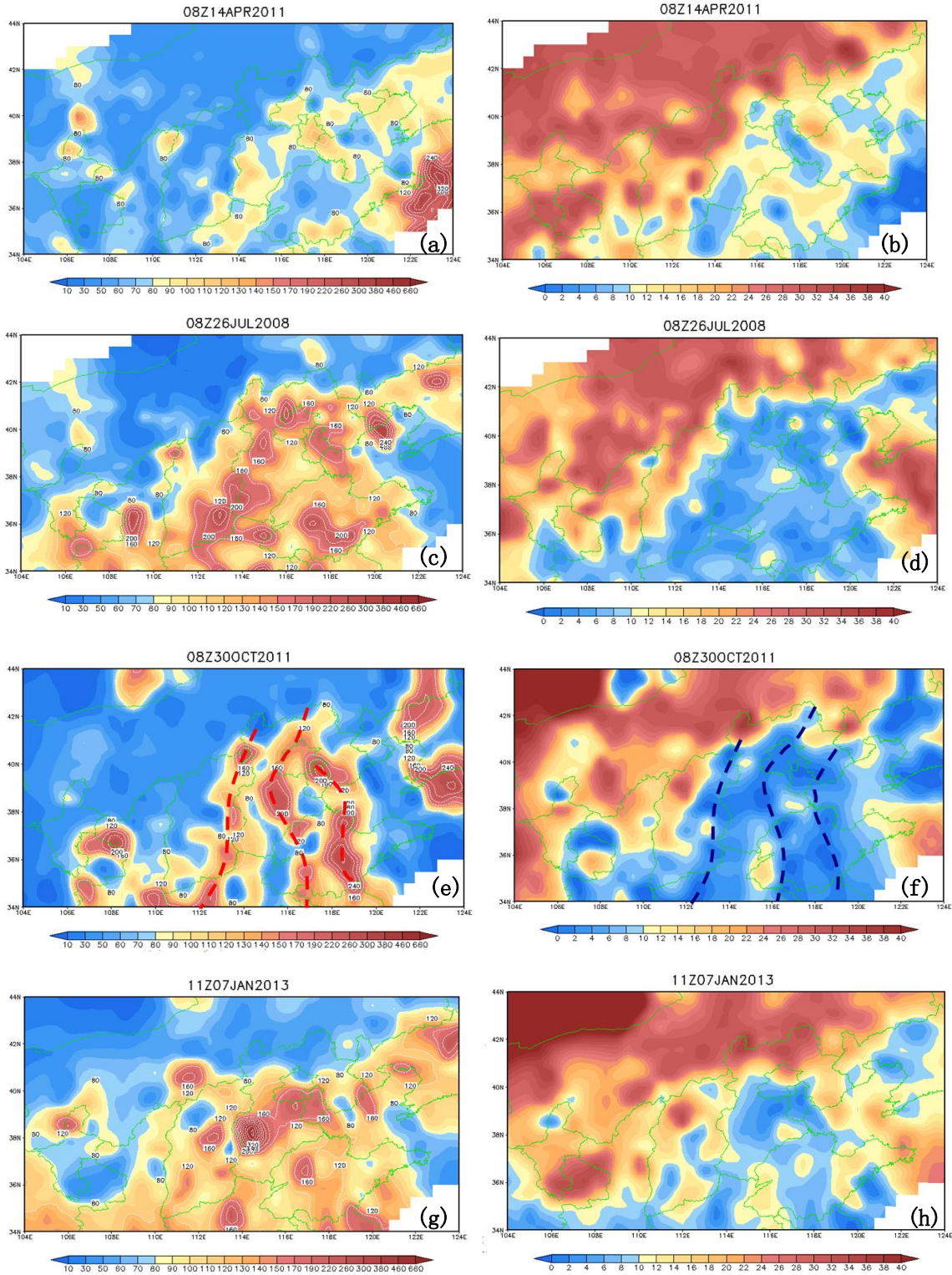
581 Figure 1 High resolution emission list E distribution (a) and its regional emission
 582 standardized list γ (b); PLAM index distribution with ignoring (c) and considering
 583 the emission condition in North China at 08:00(UTC+8) 26 February 2014



584 Figure 2 Correlation analysis of PLAM and visibility considering and not considering
 585 emission factors on 26 February 2014



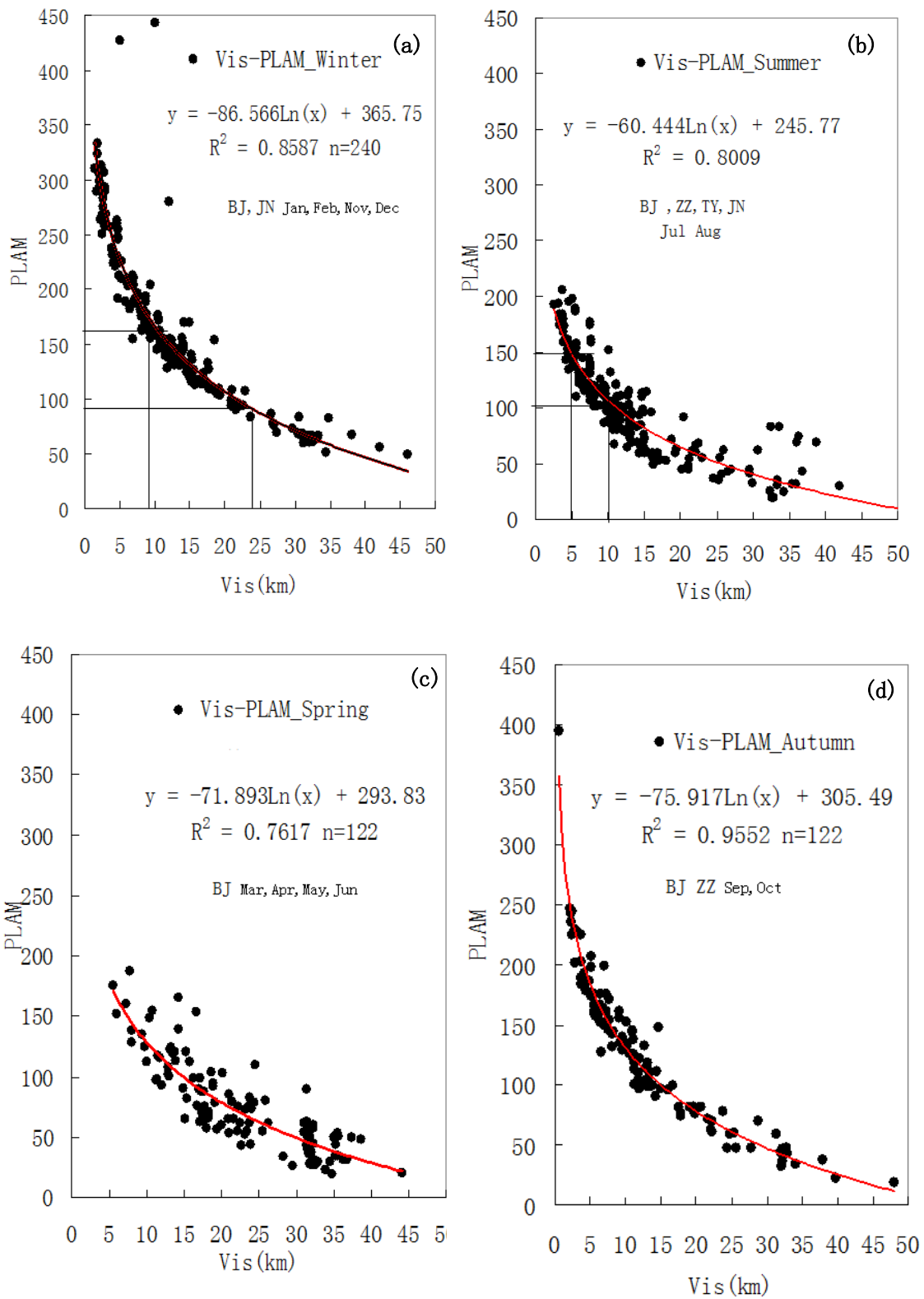
597 Figure 3 The cases for PLAM/h (a) and visibility (b) of the 14 April 2011 , PLAM/h (c)
 598 and visibility (d) of the 26 July 2008, PLAM/h (e) and visibility (f) of the 30 October
 599 2011 and PLAM/h (g) and visibility (h) on 7 January 2011



600

601

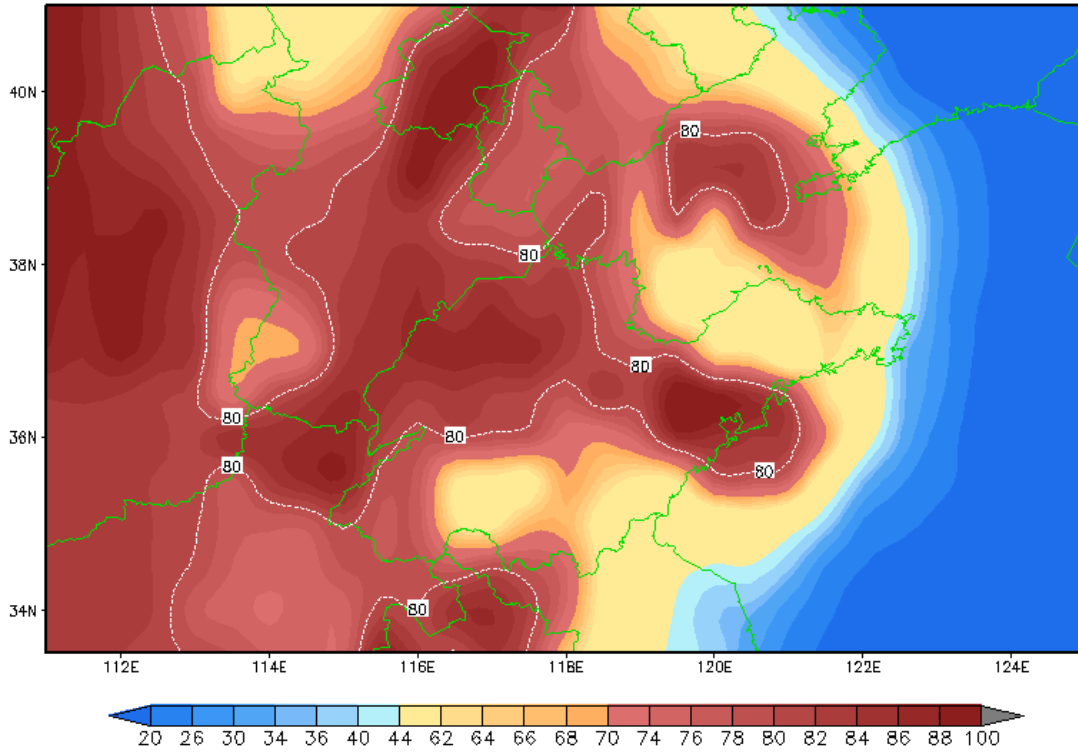
602 Figure 4 Correlation analysis of PLAM/h index and visibility in winter (a), summer (b),
 603 spring (c) and autumn (d)



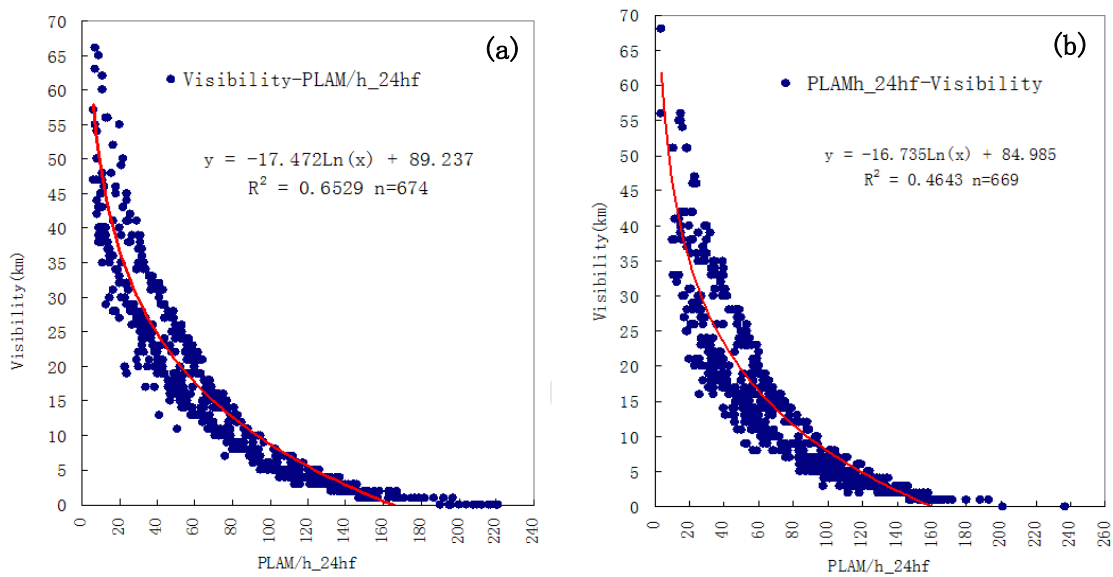
604

605

606 Figure 5 the regional correlation between PLAM/h index and visibility obtained by
 607 calculating the 1006 groups of observation samples collected from January 2009 to
 608 December 2012. The regional distribution of the correlation with significance level
 609 exceeding 0.001



610 Figure 6 the correlation analysis results of PLAM/h index 24 h forecasts and observed
 611 visibility respectively at 08:00(UTC+8) 20(a) and 08:00(UTC+8) 22(b) February



612 2014

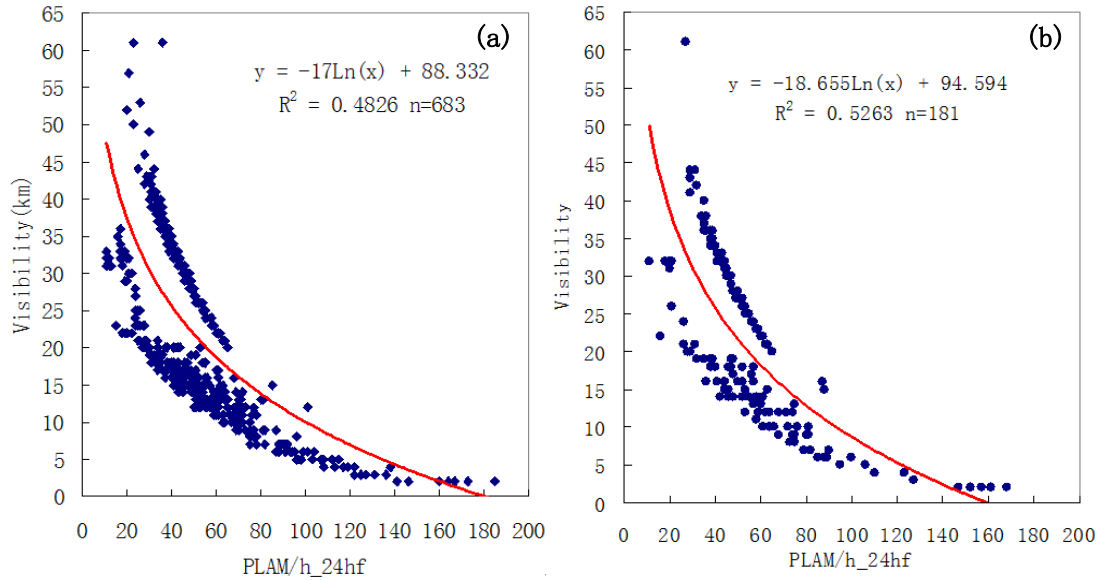
613

614

615 Figure 7 Correlation analysis of the regional PLAM/h index 24 h forecasts and
616 visibility during the whole period of pollution in North China respectively at

617 08:00(UTC+8) 20 (a) and 08:00(UTC+8) 22 July 2014(b)

618



619

620 Figure 8 distribution of PLAM/h in North China (a) and the correlation analysis of
621 PLAM/h index 24 h forecasts and observed visibility in North China for

622 8:00(UTC+8) March 12, 2014 (b)

623

624

625

626

627

628

629

630

631

632

633

